# Quantum transition processes in deformation potential interacting systems using the equilibrium density projection technique

Joung Young Sug,[1,*] Sang Gyu Jo,[2,†] Jangil Kim,[3] Jai Hoon Lee,[2,†] and Sang Don Choi[2,†]

[1]*Electronic and Electric Eng. school, Kyungpook National University, Taegu 702-701, Seoul, Republic of Korea*

[2]*Department of Physics, Kyungpook National University, Taegu 702-701, Seoul, Republic of Korea*

[3]*Department of Physics, Changwoon National University, Changwoon 643-773, Seoul, Republic of Korea*

We study cyclotron resonance line shapes (CRLS) and cyclotron resonance linewidths widths (CRLW) of deformation potential semiconductors utilizing the equilibrium density projection technique. Recently, we obtained the cyclotron resonance line-shape formula of an electron-phonon interacting system [Phys. Rev. E **60**, 66 538, (1999)]. Using this formula, we calculate numerically CRLS and CRLW. We analyze the temperature and magnetic-field dependence of CRLW in various cases. Our results agree with the experimental data obtained by H. Kobori [J. Phys. Soc. Jpn. **59**, 2141 (1990)]. Our results indicate that dominant quantum transition processes of deformation potential interacting systems are inter-Landau level transitions between the adjacent states and the effect of intra-Landau level transitions is weak. We show that most of the contribution to the total linewidth among inter-Landau level transitions comes from the transition between the excited state $\alpha = 1$ and $\beta = 0$.

## I. INTRODUCTION

The study of cyclotron resonance line shapes (CRLS) and cyclotron resonance linewidths widths (CRLW) is a useful tool for investigating the scattering mechanism of solids, since absorption line shapes and linewidths are very sensitive to the type of scattering mechanisms affecting the behavior of the carriers.

There are several methods to obtain CRLS and CRLW in response functions. Among them are the Mori, Fujita, and Suzuki methods. The Mori method uses Kubo's inner product[1] and was applied to electron-impurity systems by Kawabata to obtain CRLS.[2] Fujita expanded the CRLS formula using the proper connected diagram method and applied this method to electron-phonon systems.[3] Suzuki obtained CRLS of electron-phonon systems using the super-operator method.[4] Suzuki's theory well explains the result of Kobori group's experiment of the cyclotron resonance (CR) transition.[5–8]

Using the equilibrium density projection technique (EDPT), we have suggested a new quantum transport theory of linear-nonlinear form.[9] The merit of using EDPT is that the generalized susceptibility and scattering factor can be obtained in one step. We have also expanded the scattering factor using a continued fractional representation (CFR) to avoid the divergence problem that appears in the usual series expansion of scattering factor.[9]

In the previous work,[10] we presented a new optical conductivity formula for the CR transition in a system of electrons interacting with phonons. We summarized the calculation processes of obtaining a scattering factor using EDPT with CFR and obtained the line-shape formula of an electron-phonon interacting system.

In this paper, applying our formula in Ref. 10, we first obtain CRLS and CRLW of Ge with $\lambda = 119 \, \mu$m through numerical calculations. There are abundant experimental data[5] about the temperature dependence of CRLW[ $\gamma(T)$ ] of Ge in $\lambda = 119 \, \mu$m and the magnetic-field dependence of CRLW[ $\gamma(B)$ ] of Ge at $T = 20$ K. We compare our results of numerical calculations with existing experimental data and show a good agreement between them. This indicates that our EDPT theory is useful in analyzing many-body systems.

We analyze the temperature dependence of CRLW, $\gamma(T)$ in various wavelengths of external fields and the magnetic-field dependence of CRLW $\gamma(B)$ in various temperatures. The analysis of various cases would be difficult in other theories since they require the calculation of the absorption power to obtain CRLW. The ensemble average projection technique (EAPT) (which is contained in EDPT Ref. 9) has an advantageous aspect because we can obtain, through this technique directly, CRLW with $\gamma(T)$ and $\gamma(B)$. We do not have to calculate the absorption power to obtain CRLW.

We also analyze the quantum transition processes of deformation-potential semiconductors. Here, we confine ourselves in the inter-Landau-level transitions between the adjacent levels and the intra-Landau-level transitions within each Landau level. We characterize quantum transition processes with the $\gamma(T)$ and $\gamma(B)$ of each process and conclude that the dominant quantum transition processes of deformation-potential semiconductors occur through the inter-Landau-level transitions between the adjacent levels. The effect of intra-Landau-level transitions turns out to be weak. We further show that most of the contribution to the total linewidth among inter-Landau-level transitions comes from the transition between the excited state $\alpha = 1$ and $\beta = 0$. To the knowledge of the present authors, the analysis of CRLW and the quantum transition processes of deformation-potential semiconductors for various cases has never been done before as much as we have done here.

## II. REVIEW OF EAPT THEORY

When a circularly polarized electromagnetic wave with frequency $\omega$ and electric-field amplitude $E_0$ is incident upon

a system along the $z$ axis, the absorption power density of the electrons in solids is given by

$$P(\omega) = E_0^2 \, \mathrm{Re}\{\sigma_{\mp}(\omega)\}/2. \tag{1}$$

Here, Re represents "the real part of." We derived the conductivity tensor with weak-inter-action approximation utilizing EAPT.[10]

$$\sigma_{\mp}(\omega) = -\frac{m_l \omega_c}{2\pi^2 \hbar} \sum_{N=0}^{\infty} \int_{-\infty}^{\infty} dk_{z\alpha} \frac{i}{\hbar \omega} \frac{j_\alpha^{+2}(f_\alpha - f_{\alpha+1})}{\omega - \omega_c + i\tilde{Q}_{\mp}(\omega)}. \tag{2}$$

Here, the scattering factor $\tilde{Q}_{\mp}(\omega)$ is

$$\tilde{Q}_{\mp}(\omega) \approx iB_0 \left[ \frac{-1}{\omega\hbar^2} G0 + \frac{\frac{i}{\omega\hbar^3} G1}{i\omega + \frac{-i}{\hbar G1} G2 + \frac{-i}{\omega\hbar^2 G1} G3 + \left[\frac{-1}{\hbar G1} G2\right]^2 \Big/ \omega} \right], \tag{3}$$

where

$$GN \equiv \mathrm{Tr}\{J_- L_s (P_0 L_s)^{N+1} L_+ \rho_s\},$$

$$(N = a \; positive \; number), \tag{4}$$

$$(B_0) \equiv \frac{-1}{\mathrm{Tr}\{J_- L_+ \rho_s\}}, \tag{5}$$

and $\rho_s$ is the grand canonical density operator, Tr denotes the many-body trace for electrons, $J_{\pm}$ are the circular components of the many body current operator **J**, $L_s \equiv L_d + L_V$ is the Liouville operator corresponding to the Hamiltonian $H_s = H_d + V$, where $H_d$ and $V$ are the unperturbed and perturbed parts, respectively, and $L_+$ is the Liouville operator corresponding to the current operator $(-i/\omega)J_+$. The projection operator $P_0$ is the ensemble average projection operator that is defined as

$$P_0 X \equiv \frac{L_+ \rho_s \mathrm{Tr}\{J_- X\}}{\mathrm{Tr}\{J_- L_+ \rho_s\}}, \quad P_0' \equiv 1 - P_0, \tag{6}$$

for an arbitrary operator $X$. When a static magnetic field (**B** $= B\hat{z}$) is applied along the major axis of an ellipsoid, the Hamiltonian of the electron-phonon system is given by

$$H_s = H_d + V = H_e + H_p + V. \tag{7}$$

Here,

$$H_e = \sum_\alpha \mathcal{E}_{N_\alpha, k_{z\alpha}} a_\alpha^+ a_\alpha, \tag{8}$$

$$H_P = \sum_{\mathbf{q},s} \hbar \omega_{\mathbf{q},s} b_{\mathbf{q},s}^+ b_{\mathbf{q},s}, \tag{9}$$

and

$$V = \sum_{\mathbf{q},s} \sum_{\alpha,\mu} V_{\mathbf{q},s} \langle \alpha | \exp(i\mathbf{q}\cdot\mathbf{r}) | \mu \rangle a_\alpha^+ a_\alpha (b_{\mathbf{q},s} + b_{-\mathbf{q},s}^+); \tag{10}$$

where $a_\alpha^+ (a_\alpha)$ is the creation (annihilation) operator for an electron in the Landau state $|\alpha\rangle \equiv |N_\alpha, k_{y\alpha}, k_{z\alpha}\rangle$, $N_\alpha$ being the Landau level index, $\mathbf{k}_\alpha$ the electron wave vector, and $\mathcal{E}_{N_\alpha, k_{za}}$ the Landau energy given by

$$\mathcal{E}_{N_\alpha, k_{za}} = (N_\alpha + 1/2)\hbar \omega_c + \hbar^2 k_{z\alpha}^2 / 2m_l + \mathcal{E}_c. \tag{11}$$

Here, $\omega_c (\equiv cB/m_l)$ is the cyclotron frequency of electrons, $m_l(m_t)$ the longitudinal (transverse) effective mass of the electron, and $\mathcal{E}_c$ the bottom of the conduction band. In Eqs. (9) and (10), $b_{\pm\mathbf{q},s}^+ (b_{\pm\mathbf{q},s})$ is the creation (annihilation) operator for a phonon of energy $\hbar \omega_{\mathbf{q},s}$ in the state $|\pm\mathbf{q},s\rangle$, $\mathbf{q}$ being the phonon wave vector, $s$ the index of phonon mode, and $V_{\mathbf{q},s}$ the coupling coefficient for the electron-phonon interaction that is defined as

$$V_{\mathbf{q},s} = i(\hbar E_1 / 2\rho_m \bar{v}_s)^{1/2} \mathbf{q} \tag{12}$$

for a phonon mode $s$ where $E_1$ is the deformation-potential constant that is usually adopted as a fitting parameter when the theoretical and the experimental results are compared, $\rho_m$ is the mass density of the bulk, $\bar{v}_s$ is the average of the sound speed $v_{\mathbf{q},s}$ for each mode. The many-electron current operators $J_{\pm}$ are defined as

$$J_+ = \sum_\alpha j_\alpha^+ a_{\alpha+1}^+ a_\alpha$$

and

$$J_- = \sum_\alpha (j_\alpha^+)^* a_\alpha^+ a_{\alpha+1}, \tag{13}$$

where $j^{\pm} \equiv j_x \pm i j_v$ are two circular components of the single-electron current operator $\mathbf{j}$ and $j_\alpha^+ \equiv \langle \alpha+1 | j^+ | \alpha \rangle = ie\sqrt{2(N_\alpha+1)\hbar\omega_c/m_t}$.

With weak interaction approximation, we obtained the conductivity tensor[10] as

$$R_e \sigma_{\mp}(\omega) \equiv \frac{e^2}{\pi^2 \hbar} \left( \frac{\omega_c^2}{\omega} \right) \frac{\gamma_{\text{total}}(\omega) \int_{-\infty}^{\infty} \Delta F_\alpha dk_z}{(\omega - \omega_c)^2 + \gamma_{\text{total}}^2(\omega)}, \tag{14}$$

where the linewidth function in EAPT, which is the real part of the scattering factor, is reformulated as

$$\gamma_{\text{total}}(\omega) \approx \frac{1}{2\pi\hbar^2 v_s} \left[ \int_{-\infty}^{\infty} \int_{-\infty}^{\infty} \tilde{Y}_{\text{total}}(\omega, \omega_c, k_z, q_z, q_{\perp n}) dq_z dk_z \right] \Big/ \left[ \int_{-\infty}^{\infty} \Delta F_\alpha \right] dk_z, \tag{15}$$

with $\bar{\omega} \equiv \omega - i\eta$. Here, the function $\tilde{Y}_{\text{total}}(\omega, \omega_c, k_z, q_z, q_{\perp n})$ is defined as

$$\begin{aligned}
\tilde{Y}_{\text{total}}(\omega, \omega_c, k_z, q_z, q_{\perp n}) \equiv\ & \tilde{Y}_1^{ab}(N_\alpha, N_\beta) - \tilde{Y}_2^{ab}(N_\alpha, N_\beta) \\
& - \tilde{Y}_3^{ab}(N_\alpha, N_\beta) + \tilde{Y}_4^{ab}(N_\alpha, N_\beta) \\
& + \tilde{Y}_5^{em}(N_\alpha, N_\beta) - \tilde{Y}_6^{em}(N_\alpha, N_\beta) \\
& - \tilde{Y}_7^{em}(N_\alpha, N_\beta) + \tilde{Y}_8^{em}(N_\alpha, N_\beta),
\end{aligned} \tag{16}$$

where we classify the absorption and emission parts of phonon energy as

$$\tilde{Y}_1^{ab}(N_\alpha, N_\beta) \equiv [V(q_1)^2 q_1 K_1(N_\alpha, N_\beta; t_1) \Delta F_\alpha(n_q)]_{\beta \neq \alpha}, \tag{17}$$

$$\tilde{Y}_2^{ab}(N_\alpha, N_\beta) \equiv [V(q_2)^2 q_2 K_2(N_\alpha, N_\beta; t_2) \Delta F_{\beta, +q_z}(n_q)]_{\beta \neq \alpha}, \tag{18}$$

$$\tilde{Y}_3^{ab}(N_\alpha, N_\beta) \equiv [V(q_3)^2 q_3 K_2(N_\alpha, N_\beta; t_3) \Delta F_{\beta, +q_z}(n_q)]_{\beta \neq \alpha}, \tag{19}$$

$$\tilde{Y}_4^{ab}(N_\alpha, N_\beta) \equiv [V(q_4)^2 q_4 K_1(N_\alpha, N_\beta; t_4) \Delta F_\alpha(n_q)]_{\beta \neq \alpha+1}, \tag{20}$$

$$\tilde{Y}_5^{em}(N_\alpha, N_\beta) \equiv [V(q_5)^2 q_5 K_1(N_\alpha, N_\beta; t_5) \Delta F_\alpha(n_q+1)]_{\beta \neq \alpha}, \tag{21}$$

$$\begin{aligned}
\tilde{Y}_6^{em}(N_\alpha, N_\beta) \equiv\ & [V(q_6)^2 q_6 K_2(N_\alpha, N_\beta; t_6) \\
& \times \Delta F_{\beta, -q_z}(n_q+1)]_{\beta \neq \alpha},
\end{aligned} \tag{22}$$

$$\begin{aligned}
\tilde{Y}_7^{em}(N_\alpha, N_\beta) \equiv\ & [V(q_7)^2 q_7 K_2(N_\alpha, N_\beta; t_7) \\
& \times \Delta F_{\beta, -q_z}(n_q+1)]_{\beta \neq \alpha},
\end{aligned} \tag{23}$$

$$\begin{aligned}
\tilde{Y}_8^{em}(N_\alpha, N_\beta) \equiv\ & [V(q_8)^2 q_8 K_1(N_\alpha, N_\beta; t_8) \\
& \times \Delta F_\alpha(n_q+1)]_{\beta \neq \alpha+1},
\end{aligned} \tag{24}$$

where $t_n = \hbar q_{\perp n}^2 / 2eB$. In the above formulas, phonon wave-vectors $q_n$ are defined as $q_n \equiv \sqrt{(q_{\perp n}^2 + q_z^2)}$ with the vertical components of them $q_{\perp n}$ given by

$$q_{\perp 1} = q_{\perp 2} = \sqrt{\{[\omega + (N_\beta - N_{\alpha+1})\omega_c]v_s^{-1} + A_1(2k_{z_\alpha}q_z + q_z^2)\}^2 - q_z^2}, \tag{25}$$

$$q_{\perp 3} = \sqrt{\{[\omega + (N_\alpha - N_{\beta+1})\omega_c]v_s^{-1} - A_1(2k_{z_\alpha}q_z + q_z^2)\}^2 - q_z^2}, \tag{26}$$

$$q_{\perp 4} = \sqrt{\{[\omega + (N_\alpha - N_\beta)\omega_c]v_s^{-1} - A_1(2k_{z_\alpha}q_z + q_z^2)\}^2 - q_z^2}, \tag{27}$$

$$q_{\perp 5} = q_{\perp 6} = \sqrt{\{[-\omega - (N_\beta - N_{\alpha+1})\omega_c]v_s^{-1} + A_1(2k_{z_\alpha}q_z - q_z^2)\}^2 - q_z^2}, \tag{28}$$

$$q_{\perp 7} = \sqrt{\{[-\omega - (N_\alpha - N_{\beta+1})\omega_c]v_s^{-1} - A_1(2k_{z_\alpha}q_z - q_z^2)\}^2 - q_z^2}, \tag{29}$$

$$q_{\perp 8} = \sqrt{\{[-\omega - (N_\alpha - N_\beta)\omega_c]v_s^{-1} - A_1(2k_{z_\alpha}q_z - q_z^2)\}^2 - q_z^2}, \tag{30}$$

Here, $A_1 \equiv \hbar/2m_l v_s$. As can be seen from Eqs. (14) and (15), the integrals over the electron momentum space are done separately in numerator and denominator. Owing to the advantage of this aspect of EAPT (which is contained in EDPT Ref. 9) we can directly obtain the CRLW $\gamma$ through the integrals over phonon and electron wave-vector spaces. This allows us to analyze the temperature dependence of CRLW, $\gamma(T)$ for various wave lengths of external field, and the magnetic-field dependence of CRLW, $\gamma(B)$, at various temperatures.
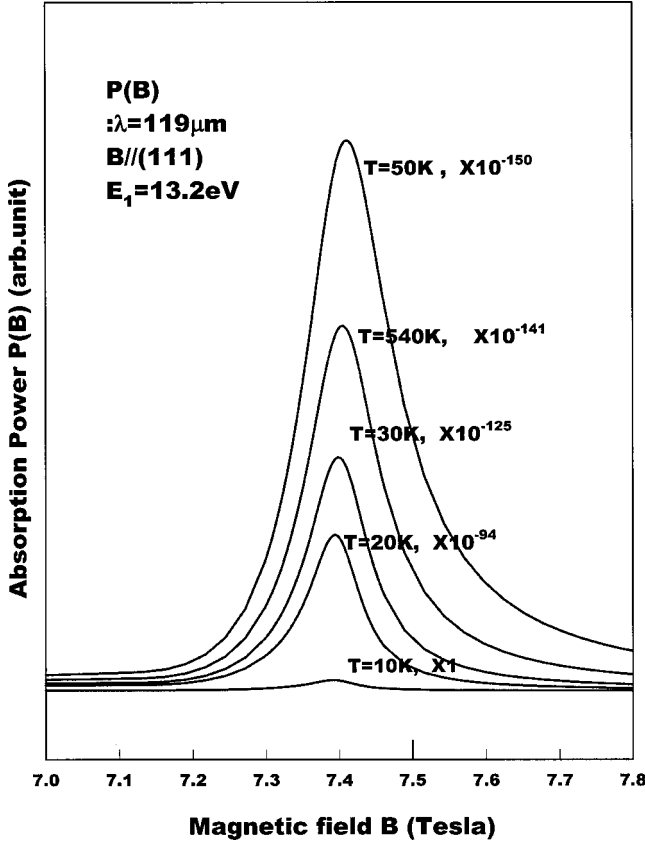
FIG. 1. The magnetic-field dependence of absorption power, $P(B)$ of Ge at $T=10$ K, $T=20$ K, $T=30$ K, $T=40$ K, $T=50$ K with $\lambda=119$ mm.

Furthermore, the above advantage of EAPT also makes it possible to analyze the quantum transition processes of deformation-potential interacting semiconductors. If we assume the interactions are weak, the effective transitions occur through the inter-Landau-level transitions between the adjacent levels, as $(\alpha,\beta)=(0,1)$ and $(\alpha,\beta)=(1,0)$, and the intra-Landau-level transitions in the same levels, as $(\alpha,\beta)=(0,0)$ and $(\alpha,\beta)=(1,1)$. In order to analyze the dominant transition among these processes, we classify the linewidths as follows.

$$\widetilde{\gamma}_{\text{total}}(\omega) \equiv \widetilde{\gamma}_{\text{intral}}(\omega) + \widetilde{\gamma}_{\text{interl}}(\omega),$$

$$\widetilde{\gamma}_{\text{intral}}(\omega) \equiv \widetilde{\gamma}_{\text{intral}}^{00,ab}(\omega) + \widetilde{\gamma}_{\text{intral}}^{00,em}(\omega) + \widetilde{\gamma}_{\text{intral}}^{11,ab}(\omega) + \widetilde{\gamma}_{\text{intral}}^{11,em}(\omega),$$

$$\widetilde{\gamma}_{\text{interl}}(\omega) \equiv \widetilde{\gamma}_{\text{interl}}^{01,ab}(\omega) + \widetilde{\gamma}_{\text{interl}}^{01,em}(\omega) + \widetilde{\gamma}_{\text{interl}}^{10,em}(\omega) + \widetilde{\gamma}_{\text{interl}}^{10,em}(\omega),$$
$$(31)$$

where

$$\widetilde{\gamma}_{\text{intral}}^{00,ab}(\omega) \equiv \frac{1}{2\pi\hbar^2 v_s} \int_{-\infty}^{\infty} \int_{-\infty}^{\infty} \widetilde{Y}_4^{ab}(0,0) dq_z dk_{z\alpha}, \quad (32)$$

$$\widetilde{\gamma}_{\text{intral}}^{11,ab}(\omega) \equiv \frac{1}{2\pi\hbar^2 v_s} \int_{-\infty}^{\infty} \int_{-\infty}^{\infty} \widetilde{Y}_4^{ab}(1,1) dq_z dk_{z\alpha}, \quad (33)$$
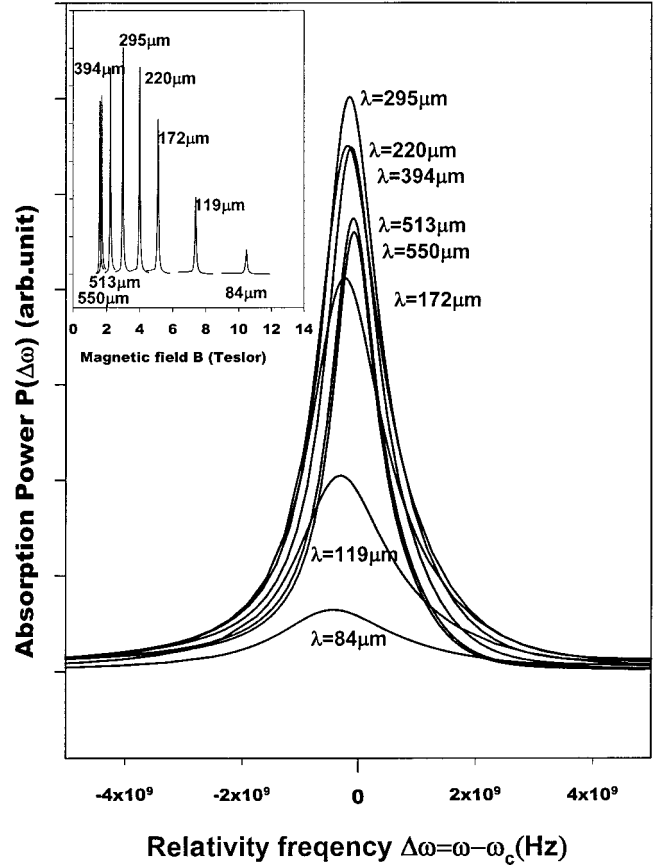


FIG. 2. The magnetic-field dependence of absorption power, $P(B)$ and $P(\Delta\omega)$ of Ge at $T=10$ K with $\lambda=84$, 119, 172, 220, 295, 394, 513, and 550 mm.

$$\widetilde{\gamma}_{\text{intral}}^{00,em}(\omega) \equiv \frac{1}{2\pi\hbar^2 v_s} \int_{-\infty}^{\infty} \int_{-\infty}^{\infty} \widetilde{Y}_8^{em}(0,0) dq_z dk_{z\alpha}, \quad (34)$$

$$\widetilde{\gamma}_{\text{intral}}^{11,em}(\omega) \equiv \frac{1}{2\pi\hbar^2 v_s} \int_{-\infty}^{\infty} \int_{-\infty}^{\infty} \widetilde{Y}_8^{em}(1,1) dq_z dk_{z\alpha}, \quad (35)$$

$$\widetilde{\gamma}_{\text{interl}}^{01,ab}(\omega) \equiv \frac{1}{2\pi\hbar^2 v_s} \int_{-\infty}^{\infty} \int_{-\infty}^{\infty} [\widetilde{Y}_1^{ab}(0,1) + \widetilde{Y}_2^{ab}(0,1)$$
$$+ \widetilde{Y}_3^{ab}(0,1)] dq_z dk_{z\alpha}, \quad (36)$$

$$\widetilde{\gamma}_{\text{interl}}^{01,ab}(\omega) \equiv \frac{1}{2\pi\hbar^2 v_s} \int_{-\infty}^{\infty} \int_{-\infty}^{\infty} [\widetilde{Y}_1^{ab}(1,0) + \widetilde{Y}_2^{ab}(1,0)$$
$$+ \widetilde{Y}_3^{ab}(1,0)] dq_z dk_{z\alpha}, \quad (37)$$

$$\widetilde{\gamma}_{\text{interl}}^{01,em}(\omega) \equiv \frac{1}{2\pi\hbar^2 v_s} \int_{-\infty}^{\infty} \int_{-\infty}^{\infty} [\widetilde{Y}_5^{em}(0,1) + \widetilde{Y}_6^{em}(0,1)$$
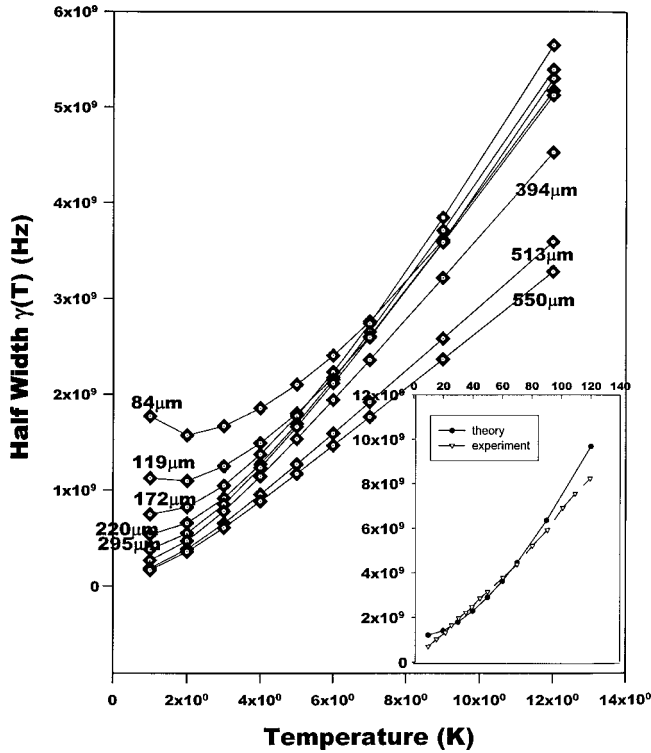$$+ \widetilde{Y}_7^{em}(0,1)] dq_z dk_{z\alpha}, \quad (38)$$

FIG. 3. The temperature dependence of half line width, $\gamma(T)$ of Ge with $\lambda$ = 84, 119, 172, 220, 295, 394, 513, and 550 $\mu$m. In small box, we compare the theoretical result with experimental data of the temperature dependence of half line width, $\gamma(T)$ of Ge with $\lambda$ = 119 $\mu$m.
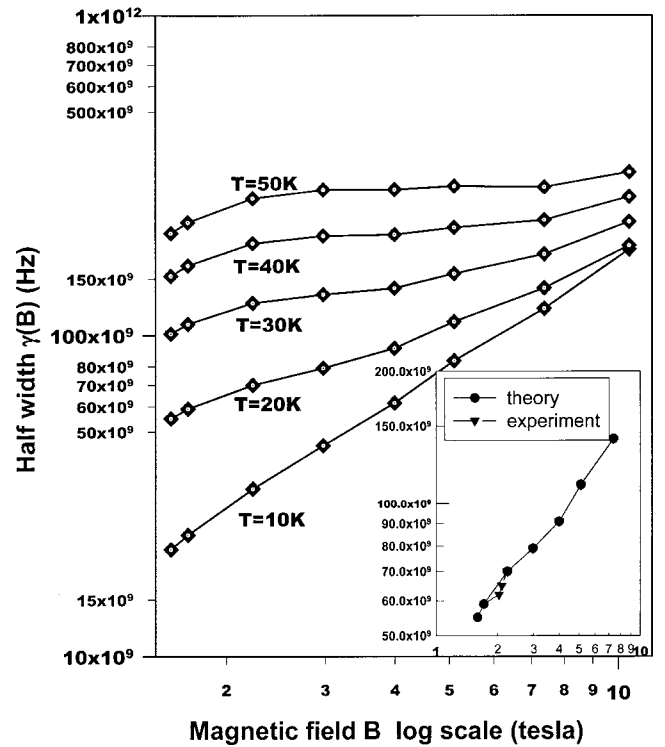


FIG. 4. The magnetic-field dependence of half line width, $\gamma(B)$ of Ge at $T$ = 10, 20, 30, 40, and 50 K. In small box, we compare the theoretical result with experimental data of the magnetic-field dependence of half line width, $\gamma(B)$ of Ge at $T$ = 20 k.

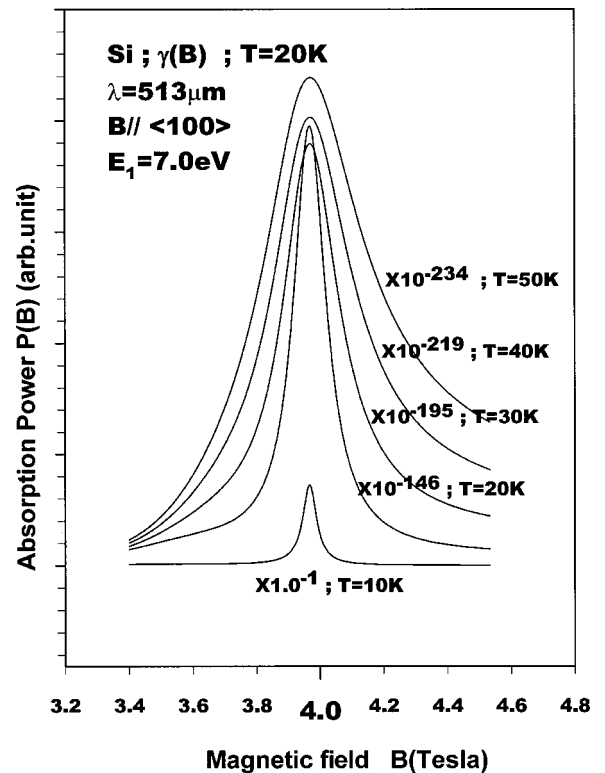$$\widetilde{\gamma}_{\text{interl}}^{10,\text{em}}(\omega) \equiv \frac{1}{2\pi\hbar^2 v_s} \int_{-\infty}^{\infty}\int_{-\infty}^{\infty} [\widetilde{Y}_5^{\text{em}}(1,0) + \widetilde{Y}_6^{\text{em}}(1,0)$$

$$+ \widetilde{Y}_7^{\text{em}}(1,0)]dq_z dk_{z\alpha}. \qquad (39)$$

## III. THE ABSORPTION POWERS AND THE LINEWIDTHS OF EAPT IN CR TRANSITION

In this section, we calculate the linewidths of Ge and Si in the quantum limit. It is well known that the deformation-potential scattering is dominant for pure Ge and Si. The band structure of Ge and Si can be approximated to be ellipsoidal.

For $\mathbf{B}\|\langle 111\rangle$ in Ge we have $m_l = 0.22m_0$ and $m_l = 0.35m_0$ where $m_0$ is the free-electron mass. The other constants are $\rho = 5.36$ g/cm$^3$, $s = 5.94\times10^5$ cm/s, $\mathcal{E}_g(0) = 0.744$ eV, $\kappa = 4.77\times10^{-4}$ eV/K and $\xi = 235$ K. Inserting these constants into Eqs. (1), (7), (13), and (14) and carrying out the integration in Eq. (11), we obtain the line shapes, from which the width can be measured.

It is known that as for the cyclotron resonance, there are abundant experimental data[5] concerning the temperature dependence of CRLW[$\gamma(T)$] of Ge in $\lambda = 119$ $\mu$m and the magnetic-field dependence of CRLW[$\gamma(B)$] of Ge at $T = 20$ K. In order to examine the validity of our theory, we first compare our EAPT theory with the experimental data through the numerical calculations. In Fig. 1, we obtain the power absorptions, $P(B)$ of Ge with $\lambda = 119$ $\mu$m at $T$



FIG. 5. The magnetic-field dependence of absorption power, $P(B)$ of Si at $T = 10$ K, $T = 20$ K, $T = 30$ K, $T = 40$ K, $T = 50$ K with $\lambda = 513$ mm.
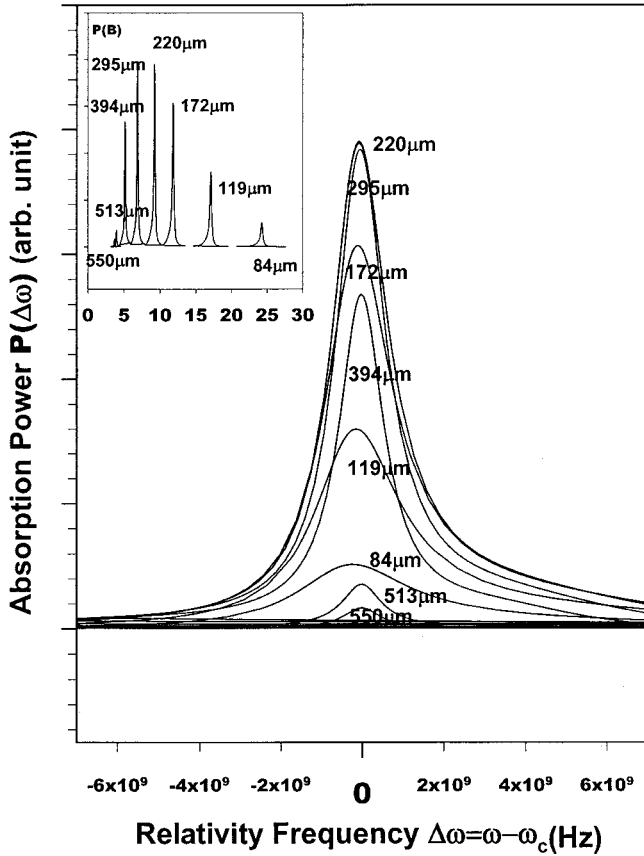
FIG. 6. The magnetic-field dependence of absorption power, $P(B)$ and $P(\Delta\omega)$ of Si at $T=10$ K, with $\lambda=84$, 119, 172, 220, 295, 394, 513, and 550 $\mu$m.

$=10$ K, $T=20$ K, $T=30$ K, $T=40$ K, $T=50$ K. The shape of $P(B)$ resembles the experimental shape of $P(B)$ with an arbitrary unit performed by Kobori *et al.* In Fig. 2, we obtain the power absorptions, $P(B)$ and $P(\Delta\omega)$ of Ge at $T=10$ K with $\lambda=84\,\mu$m, $\lambda=119\,\mu$m, $\lambda=172\,\mu$m, $\lambda=220\,\mu$m, $\lambda=295\,\mu$m, $\lambda=394\,\mu$m, $\lambda=513\,\mu$m, and $\lambda=550\,\mu$m. Here, $\Delta\omega=\omega-\omega_0$. From the graph of $P(\Delta\omega)$, we can see the broadening effects near the resonance peaks for various external fields. The graph in the small box indicates the locations of resonance peaks for various external fields. We can read from this graph the magnetic-field dependence of the maximum absorption power. In Fig. 3, we obtain the temperature dependence of linewidths of Ge with $\lambda=84$, 119, 172, 220, 295, 394, 513, and 550 $\mu$m. The advantage of EAPT theory is evident in the calculation of linewidths for various cases. It would be cumbersome with other theories. In the small box, we plot both the linewidths coming from the EAPT theoretical result and Kobori's experimental result for the case with $\lambda=119\,\mu$m. We see a good coincidence between them. They both show rising behaviors as temperature increases.

In Fig. 4, we obtain the magnetic-field dependence of linewidths of Ge at $T=10$, 20, 30, 40, and 50 K. In the small box, we compare the theoretical result with the experimental data for the case when $T=20$ K. Again, we see a good agreement between them. We want to emphasize here again that it is easier than other theories to obtain the line-
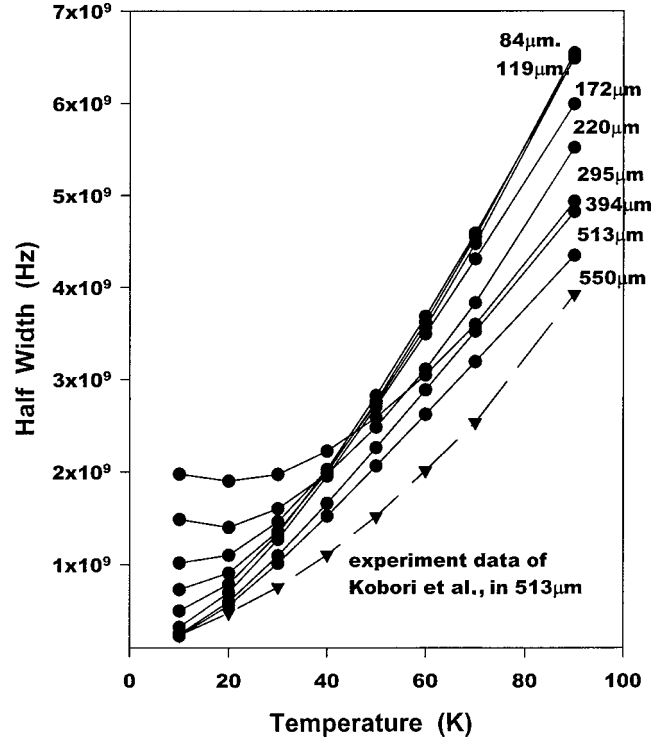
widths because they can be obtained directly in EAPT theory.

Now for Si, we have $m_t=0.33\,m_o$, $m_l=0.58\,m_o$, $\rho=2.34$ g/cm$^3$, $s=9.03\times10^5$ cm/s, $\mathcal{E}_g(0)=1.17$ eV, $\kappa=$



FIG. 7. The temperature dependence of half line width, $\gamma(T)$ of Si with $\lambda=84$, 119, 172, 220, 295, 394, 513, 550 $\mu$m.
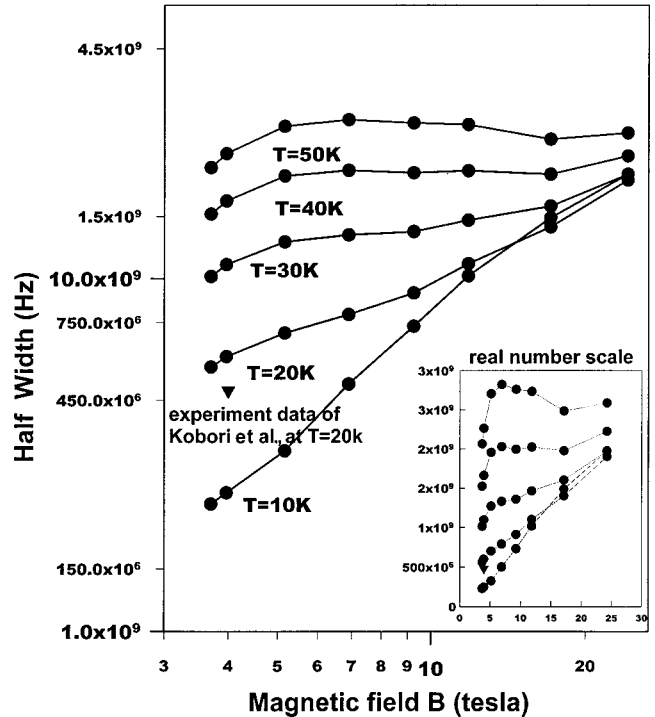


FIG. 8. The magnetic-field dependence of half line width, $\gamma(B)$ of Si at $T=10$, 20, 30, 40, and 50 k.
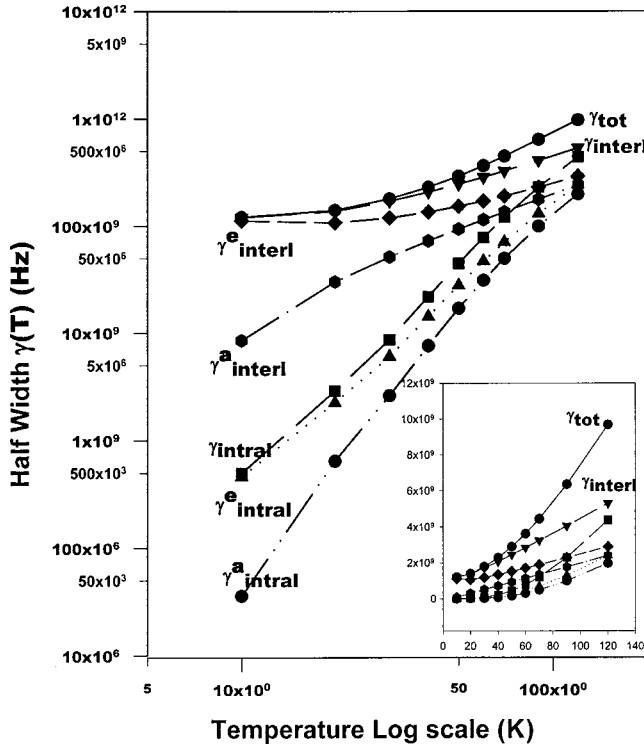
FIG. 9. The temperature dependence of linewidth of Ge in cases of total line width ($\gamma_{tot}$), total inter Landau level($\gamma_{interl}$), total intra-Landau level($\gamma_{intral}$), phonon emission inter-Landau level($\gamma_{interl}^{e}$), phonon emission intra-Landau level($\gamma_{intral}^{e}$), phonon asorption inter-Landau level($\gamma_{interl}^{a}$), and phonon asorption intra-Landau level($\gamma_{intral}^{a}$) transition.

$4.73 \times 10^{-4}$ eV/K, and $\xi = 636$ K, $E_1 = 9.3$ eV. In Fig. 5, we obtain the power absorptions, $P(B)$ of Si with $\lambda = 513$ $\mu$m at $T = 10, 20, 30, 40, 50$ K. In Fig. 6, we obtain the power absorptions, $P(B)$ $P(\Delta\omega)$ of Si at $T = 20$ K with $\lambda = 84, 119, 172, 220, 295, 394, 513, 550$ $\mu$m. We see that the general shape of power absorptions of Si is very similar to that of Ge. In Fig. 7, we show the temperature dependence of linewidths of Si for various $\lambda$'s. In Fig. 8, we obtain the magnetic field dependence of linewiths of Si at various temperatures. In Figs. 7 and 8, we included some experimental data. Note that there are not abundant experimental data of Si compared to Ge. The agreement between EAPT theoretical predictions and experimental results for Si case is not as good as the case of Ge. Nevertheless, the discrepancy is in the range of acceptance.

The results of this section indicate that our EAPT theory well accepts Kobori's experimental data.[5] Therefore, we confirm that the EAPT theory is quite useful to understand the scattering mechanism in CR transition. We expect it can be applied to analyses of other condensed material systems.

## IV. THE TRANSITION PROCESSES IN CR TRANSITION WITH EAPT

Since we can obtain the CRLW, $\gamma(T)$ and $\gamma(B)$ directly from the numerical calculations in EAPT theory, we can analyze easily $\gamma(T)$ in various wavelengths of external fields
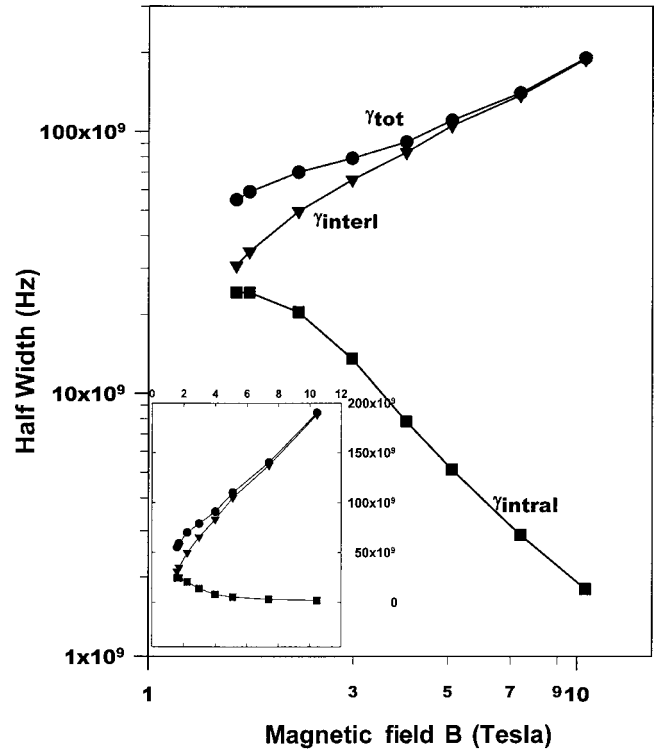


FIG. 10. The magnetio-field dependence of linewidth of Ge in cases of total line width ($\gamma_{tot}$), total inter-Landau level($\gamma_{interl}$), and total intra-Landau level($\gamma_{intral}$) transition.

$gamma(B)$ in various temperatures. Further anaysis of various cases are performed in this section. In Fig. 9, we plot the temperature dependence of linewidths of Ge for various transitions. They include inter-Landau-level transition and intra-Landau-level transition, each of which is further separated into two cases, phonon-absorption transition and phonon-emission transition. We denote the total linewidth as $\gamma_{tol}$, the inter-Landau-level linewidth as $\gamma_{inter-l}(T)$, the intra-Landau-level linewidth as $\gamma_{inter-l}(T)$, the phonon-absorption inter-Landau-level linewidth as $\gamma_{inter-l}^{a}(T)$, the phonon-emission inter-Landau-level linewidth as $\gamma_{intra-l}^{e}(T)$, the phonon-absorption intra-Landau-level linewidth as $\gamma_{intra-l}^{a}(T)$, and the phonon-emission intra-Landau-level linewidth as $\gamma_{intra-l}^{e}(T)$. From these graphs we read that the broadening effect is dominated by the phonon-emission inter-Landau-level transition at low temperature. In Figs. 10 and 11, we plot the magnetic-field dependence of linewidths of Ge for various transitions at $T = 20$ K. Here again, we read that the broadening effect is dominated by the phonon-emission inter-Landau-level transition. In Fig. 12, we plot the magnetic-field dependence of linewidths of Si for various transitions at $T = 20$ K. From these results, we observe similarities between quantum transition properties of Ge and Si.

## V. CONCLUSIONS

In this paper, we studied cyclotron resonance line shapes (CRLS) and cyclotron resonance linewidths widths (CRLW) of deformation-potential semiconductors using EAPT theory.
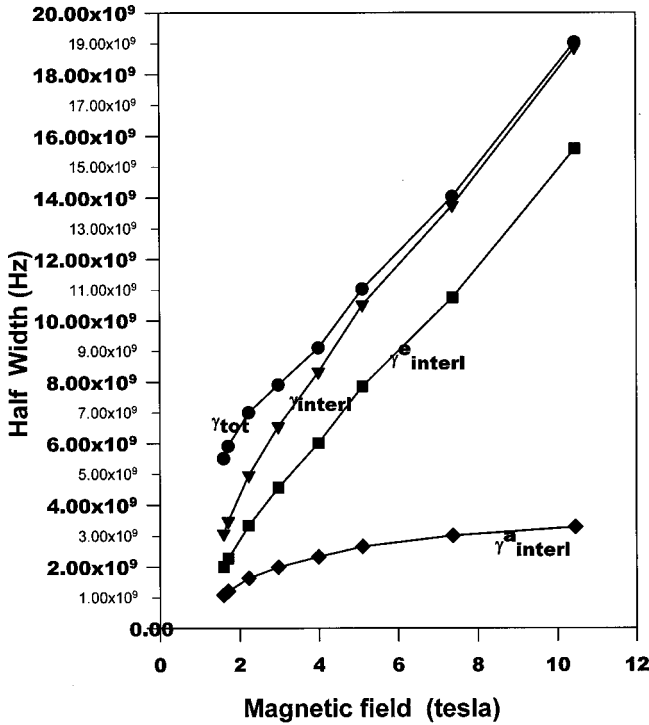
FIG. 11. The magnetic-field dependence of linewidth of Ge in cases of total line width ($\gamma_{tot}$), total inter-Landau level($\gamma_{interl}$), phonon emission intra-Landau level($\gamma_{interl}^{e}$), and phonon absorption intra-Landau level($\gamma_{interl}^{a}$) transition.



FIG. 12. The magnetic-field dependence of linewidth of Si in cases of total line width ($\gamma_{tot}$), total inter-Landau level($\gamma_{interl}$), and total intra-Landau level($\gamma_{intral}$) transition.

We compare the EAPT theoretical predictions with experimental data of H. Kobori *et al.* Our results of numerical calculations appear to be reasonable since $\gamma(T)$ of Ge in $\lambda = 119\,\mu$m and $\gamma(B)$ of Ge in $T = 20$ K agree well with the experimental results.[5] This indicates that the EAPT theory is quite useful to understand the scattering mechanism in CR transition.

We analyzed the temperature dependence of CRLW$\gamma(T)$ in various wavelengths of external fields, and the magnetic-field dependence of CRLW$\gamma(B)$ in various temperatures. We want to emphasize that our EAPT theory makes these analyses of various cases much easier than other theories, since more steps are involved in the calculations in other theories.

The EAPT theory enables us to separate the linewidths in terms of each quantum transition for various cases. The results are plotted in Figs. 9–12. From these graphs, we get the
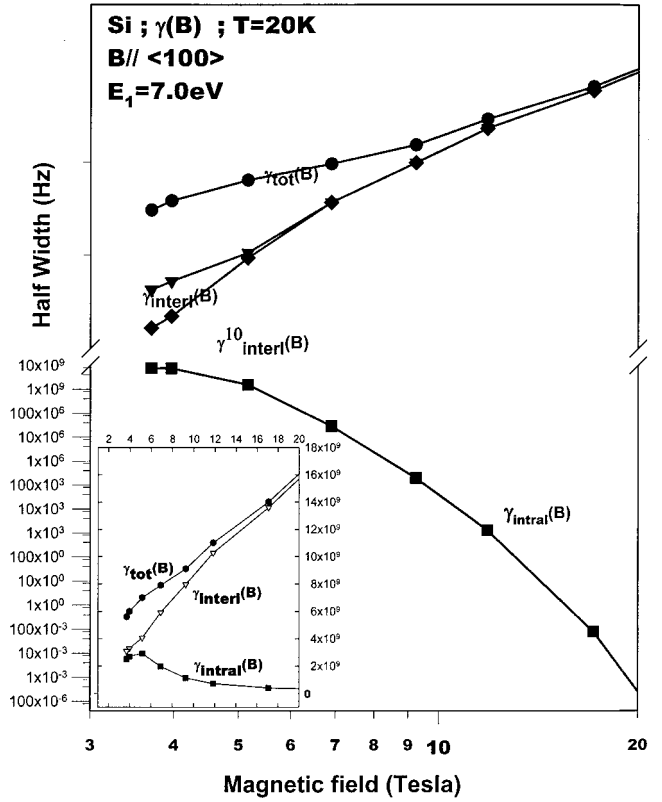
following properties. First, the temperature dependence of linewidths of Ge is dominated by the phonon-emission inter-Landau-level transition at low temperature. Second, the magnetic-field dependence of linewidths of Ge is also dominated by the phonon-emission inter-Landau-level transition. Third, the same properties apply to the case of Si. From these results, we observe similarities between quantum transition properties of Ge and Si. The easy analysis of each quantum transition processes are the merits of our EAPT theory. Finally, we expect that the EAPT (or EDPT) theory is also useful in other condensed material systems.

*FAX: 82-053-950-6614; Email address: jysug@bh.knu.ac.kr

†FAX: 82-053-952-1739; Email address: sgjo@bh.knu.ac.kr

[1] R. Kubo, J. Phys. Soc. Jpn. **12**, 570 (1957).

[2] H. Mori, Prog. Theor. Phys. **33**, 423 (1965); **34**, 399 (1966); M. Tokuyama and H. Mori, *ibid.* **55**, 2 (1975); A. Kawabata, J. Phys. Soc. Jpn. **23**, 999 (1967); K. Nagano, T. Karasudani, and H. Okamoto, Prog. Theor. Phys. **63**, 1904 (1980).

[3] S. Fujita and C. C. Chen, Int. J. Theor. Phys. **2**, 59 (1969); S. Fujita and R. Hirota, Phys. Rev. **118**, 6 (1968); S. D. Choi and S. Fujita, Solid State Commun. **37**, 293 (1981).

[4] A. Suzuki and D. Dunn, Phys. Rev. B **25**, 7754 (1982).

[5] Otsuka, T. Ohyama, and K. Murase, J. Phys. Soc. Jpn. **25**, 729 (1968); H. Kobori, T. Ohyama, and E. Otsuka, *ibid.* **59**, 2141 (1989); H. Kobori, *ibid.* **59**, 2164 (1989).

[6] P. N. Argres and J. L. Sigel, Phys. Rev. Lett. **31**, 1397 (1973); P. N. Argyres and J. L. Sigel, Phys. Rev. B **10**, 139 (1974).

[7] S. D. Choi and O. H. Chung, Solid State Commun. **46**, 717 (1983); S. N. Yi, J. Y. Ryu, O. H. Chung, J. Y. Sug, and S. D. Choi, Nuovo Cimento D **9**, 927 (1987); Y. J. Lee, S. D. Choi, S. N. Yi, J. Korean Phys. Soc. **27**, 195 (1994); J. Y. Ryu, S. N. Yi,

and S. D. Choi, J. Phys. C **2**, 3515 (1990); Youn Ju Lee, Y. J. Cho, C. H. Choi, Joung Young Sug, and S. D. Choi, Z. Phys. B: Condens. Matter **98**, 55 (1995); N. L. Kang, Y. J. Cho, and S. D. Choi, J. Korean Phys. Soc. **29**, 628 (1996); J. Y. Sug, S. G. Cho, S. D. Choi, *ibid.* **34**, 135 (1999).

[8] T. Ando and Y. Uemura, J. Phys. Soc. Jpn. **36**, 959 (1974); X. Wu and F. M. Peeters, Phys. Rev. B **41**, 3109 (1990).

[9] J. Y. Sug and S. D. Choi, Phys. Rev. E **55**, 314 (1997).

[10] J. Y. Sug, S. G. Jo, and S. D. Choi, Phys. Rev. E **60**, 6538 (1999).